

## Dinoflagellate cysts as indicators of climatic and oceanographic changes during the past 40 kyr in the Santa Barbara Basin, southern California

Vera Pospelova,<sup>1</sup> Thomas F. Pedersen,<sup>1</sup> and Anne de Vernal<sup>2</sup>

Received 26 November 2005; revised 22 January 2006; accepted 8 February 2006; published 9 May 2006.

[1] The dinoflagellate cyst record from Ocean Drilling Program Hole 893A, Santa Barbara Basin, southern California, is examined at millennial-scale resolution for the past ~40 kyr. Changes in cyst abundance, composition of cyst assemblages, and their diversity reflect major shifts in climate and ocean circulation in the region over this time interval. Throughout the sequence, dinoflagellate cyst assemblages are dominated by heterotrophic dinoflagellates. *Brigantedinium* spp. and other upwelling-related taxa such as *Echinidinium* and *Protoperidinium americanum* are abundant, indicating the continued influence of coastal upwelling on the basin during the late Quaternary. A significant increase in cyst accumulation rates is seen during the Holocene and, to a lesser extent, during shorter warming events such as Bolling/Allerod and Dansgaard-Oeschger interstadials, implying enhanced marine productivity during these periods. Cyst diversity is high during the Holocene. An increase in abundance of cysts produced by autotrophic dinoflagellates in the late Holocene suggests enhanced input of warm, nutrient-rich waters. In contrast, cyst assemblages from the Last Glacial Maximum exhibit a relatively low diversity and an increase in the cysts of heterotrophic dinoflagellates, in particular *Selenopemphix nephroides*. The presence of this taxon in association with *Brigantedinium* spp. implies substantial cooling of surface waters in the Santa Barbara Basin at that time.

**Citation:** Pospelova, V., T. F. Pedersen, and A. de Vernal (2006), Dinoflagellate cysts as indicators of climatic and oceanographic changes during the past 40 kyr in the Santa Barbara Basin, southern California, *Paleoceanography*, 21, PA2010, doi:10.1029/2005PA001251.

### 1. Introduction

[2] Previously published paleoceanographic records from ODP Hole 893, drilled in the Santa Barbara Basin (SBB) on the southern Californian borderlands, have provided detailed information on late Quaternary climate variability and the intensity of the upwelling in the region. Extensive geochemical and microfossil studies of Core 893A have yielded several important findings. *Behl and Kennett* [1996], for example, observed that the warm interstadial Dansgaard-Oeschger (DO) events recorded in Greenland ice cores and in North Atlantic sedimentary records are imprinted in the SBB sediments as a sequence of laminated layers deposited under anoxic conditions. The same events were identified in down core planktonic and benthic foraminiferal census data [*Hendy and Kennett*, 1999, 2000; *Hendy et al.*, 2002], in foraminiferal oxygen isotope ( $\delta^{18}\text{O}$ ) records for both surface and thermocline-dwelling taxa, and in shifts in the composition of foraminiferal assemblages. Such data have yielded insights on the regional response to variations in the strength of the California Current, the

intensity of upwelling, local temperature fluctuations, and changes in deepwater ventilation in the SBB.

[3] This work adds to the existing body of paleoceanographic information by presenting a millennial-scale analysis of the dinoflagellate cyst record in the SBB over the last 40 kyr. Dinoflagellates, one of the principal groups of marine phytoplankton, have a life cycle that includes a cyst stage. Contrary to live dinoflagellates, cysts have highly resistant organic walls that are in general well preserved in marine sediments. Although certain cyst taxa may be affected by oxidization [*Dale*, 1976; *Zonneveld et al.*, 1997] the dinoflagellate cyst record provides important information where other mineralized microfossil taxa, such as foraminifera, diatoms, and radiolaria, are subject to dissolution.

[4] The distribution of dinoflagellate cysts in surface sediments have been shown to correlate with physical characteristics of overlying surface water masses [*Wall et al.*, 1977; *de Vernal et al.*, 1994; *Dale*, 1996; *Rochon et al.*, 1999], even on relatively fine spatial scales [*Pospelova et al.*, 2004, 2005]. Hence cysts can be used for reconstructions of paleoenvironmental conditions, including sea surface temperature and productivity. Studies of dinoflagellate cysts along the Pacific margin of North America are relatively rare, and have primarily focused on modern/recent sediments [*Kumar and Patterson*, 2002; *Mudie et al.*, 2002; *Prauss*, 2002; *Radi and de Vernal*, 2004]. The only studies of dinoflagellate cysts in the North Pacific that span glacial and interglacial periods were conducted in the

<sup>1</sup>School of Earth and Ocean Sciences, University of Victoria, Victoria, British Columbia, Canada.

<sup>2</sup>Centre de recherche en géochimie isotopique et en géochronologie (GEOTOP), Université du Québec à Montréal, Montréal, Québec, Canada.

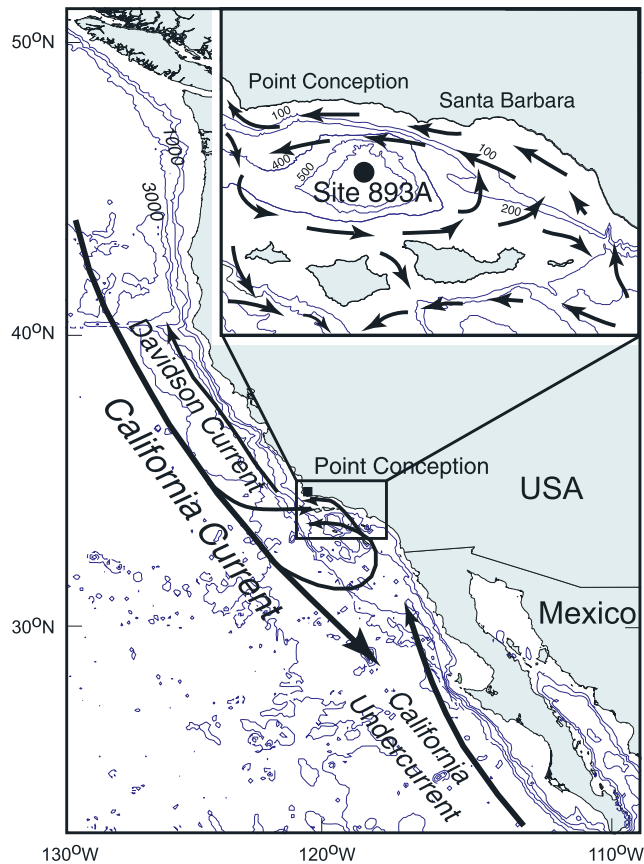


**Figure 1.** Map showing the location of ODP Hole 893A in the Santa Barbara Basin, bathymetry (meters) and surface ocean currents on the southern California continental margin.

Gulf of Alaska by *de Vernal and Pedersen* [1997] and *Marret et al.* [2001] where a quantitative reconstruction of the SST was performed using the modern analogue techniques.

[5] Recent work by *Radi and de Vernal* [2004] explored the spatial distribution of dinoflagellate cysts and environmental conditions in the Gulf of Alaska and along the British Columbia and Oregon coasts. Their results have highlighted the importance of seasonal upwelling intensity on cyst export to the underlying sediments. Cysts produced by heterotrophic dinoflagellates, in particular by the genus *Protoperidinium*, dominate cyst assemblages in these productive regions and can be used as an indicator of active upwelling. Such observations appear to be universal: *Reichert and Brinkhuis* [2003] for example, found that changes in the relative abundance and concentrations of *Protoperidinium* cysts in the Arabian Sea correlate with major climatic events in the late Quaternary and reflect changes in paleoproductivity. A similar signal could be

anticipated in the sedimentary dinoflagellate cyst record along the upwelling margin of southern California.

[6] We document here variations in dinoflagellate cyst abundance and species composition at approximately millennial-scale intervals in the Santa Barbara Basin over the last 40 kyr. Our objectives are as follows: (1) to explore the utility of dinoflagellate cysts in mapping both low- and high-frequency climatic changes in this oceanographic setting; (2) to compare changes so defined with variations observed in other paleoproxies; and (3) to shed additional light on climatic and oceanographic history in the region.

## 2. Environmental Setting

[7] The Santa Barbara Basin is a ~600-m-deep semi-enclosed basin located at the northern end of Southern California Bight on the Northeast Pacific margin (Figure 1). It is separated from the Southern California Bight by several Channel Islands to the south and by a ~230 m sill to the east [*Emery, 1960*]. An approximately 475 m deep sill restricts water circulation between the SBB and the open ocean to the west. Below sill depth, the basin contains oxygen-depleted waters that foster preservation of laminated sediments.

[8] The hydrology of the Santa Barbara Basin is dominated by the California Current System, which comprises the California Current (CC), the Davidson Current and the California Undercurrent [*Hickey, 1998*]. The California Current transports relatively cold subarctic waters high in dissolved oxygen and nutrients southward along the Pacific coast of the United States up to 1000 km offshore, from the Washington-Oregon border to southern California. South of Point Conception, a portion of the CC turns southeastward, then shoreward and northward to become the Southern California Countercurrent or Southern California Eddy. Point Conception generally separates the colder waters of the California Current from the warmer waters circulating in the Santa Barbara Channel.

[9] The California Undercurrent is a relatively narrow countercurrent that flows over the continental slope northward from Baja. The flow originates in the eastern equatorial Pacific and carries warmer, more saline and nutrient-rich but oxygen poor water to the north. The Davidson Current is a seasonal surface flow that runs northward over the shelf zone from Point Conception to Vancouver Island during the fall and winter. It has been suggested that this current is a result of the California Undercurrent surfacing in the fall when the CC weakens [*Pavlova, 1966; Huyer and Smith, 1974*].

[10] Upwelling peaks in the summer, when northerly winds are at a seasonal maximum [*Lynn and Simpson, 1987*]. The winds intensify the south-flowing California Current, enhancing input of less saline, cold upwelling waters from north of Point Conception to the Santa Barbara Basin. In winter, when northerly winds weaken, the intensified California Undercurrent enhances input of warm, saline, oxygen poor and nutrient rich waters from the south.

**Figure 2.** Relative abundance of dinoflagellate cyst taxa that contribute more than 1% to the cyst assemblages. Solid dots indicate rare occurrences (1.5% or less). Diagram shows position of the sample used in this study and total cyst counts on the right, as well as dinoflagellate cyst zones and PCA values on the left.

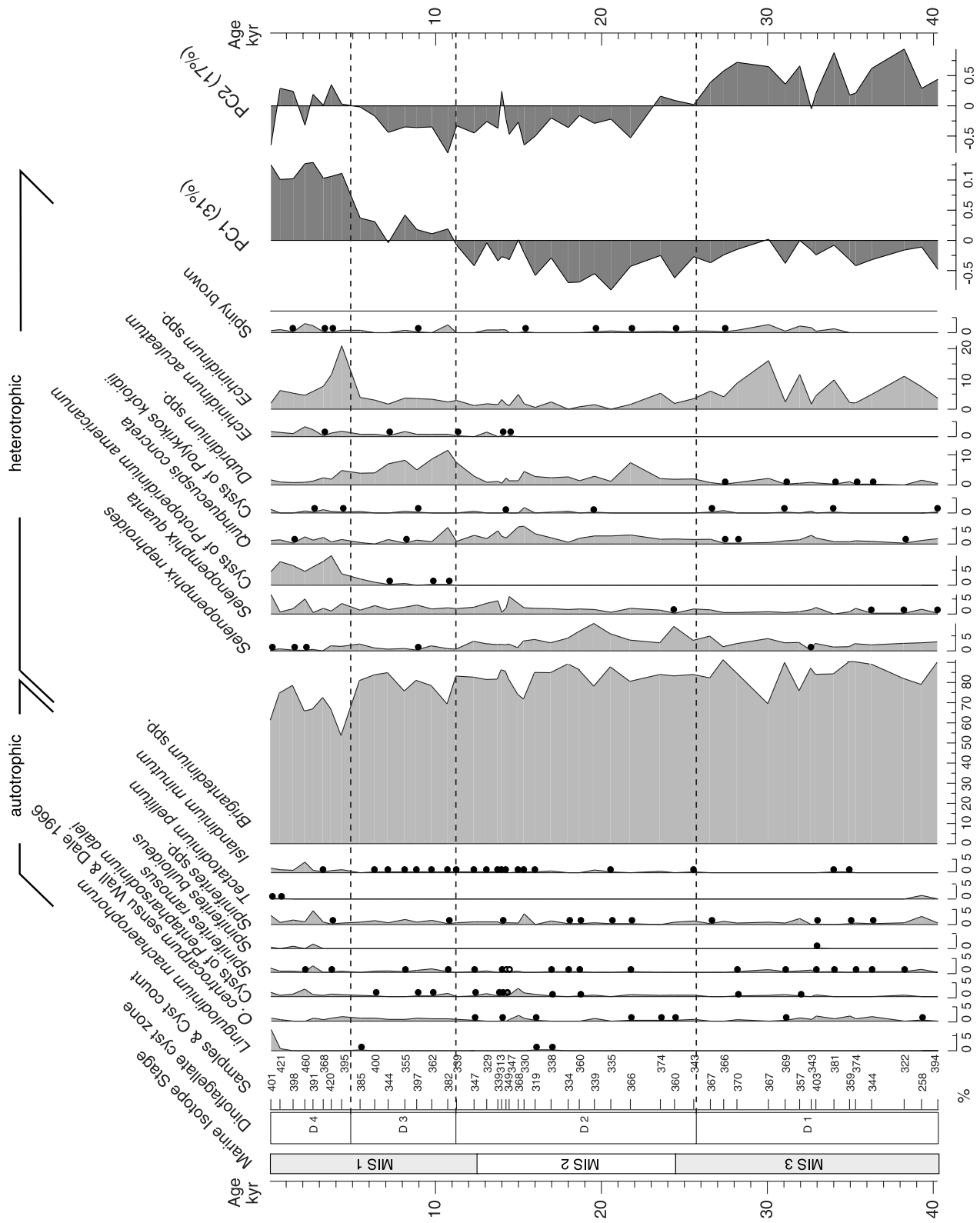


Figure 2

In addition, episodic “flushing events” replace deep waters of the Santa Barbara Basin with cool, nutrient-rich, oxygen-depleted waters derived from North Pacific Intermediate Water to the west.

### 3. Material and Methods

[11] Ocean Drilling Program (ODP) Leg 146 Hole 893A (Latitude: 34°17.25'N; Longitude: 120°2.2'W) was drilled in 1992 at 576.5 m water depth, in the deepest part of the central Santa Barbara Basin (Figure 1). The 196.5 m section recovered spans the late Quaternary from 160 kyr to the present. The sedimentary sequence consists of olive-gray clay and silt with a few sand layers and is characterized by repeated intercalations of bioturbated and laminated strata [Behl, 1995].

[12] The chronology used in this study was developed by Behl and Kennett [1996] and is based on varve counting for the top 10 kyr and AMS <sup>14</sup>C ages of planktonic foraminifera for the remaining section of the core (the last 40 kyr).

[13] Samples were selected from the upper 59 m of the core, sections 1H to 7H of ODP Hole 893A. Forty-nine sediment samples were subsampled at ~1 m intervals for dinoflagellate cyst analyses (Figure 2). Sampling intervals between the samples correspond to 0.08–1.8 kyr of deposition, with an average of 0.8 kyr.

[14] Dinoflagellate cysts, foraminiferal organic linings (thin inner organic layer of some foraminifera that resist acidic dissolution), pollen grains and spores were recovered using the following procedure. Samples of known volume were oven-dried at 40°C, rinsed twice with distilled water, and sieved through 125 µm and retained on 10-µm mesh to eliminate coarse and fine material. Additions of 40% hydrofluoric acid (HF) for up to 3 days and 10% HCl for 30 min removed siliceous phases and carbonates. The residue was then rinsed twice with distilled water, sonicated for between 0.5 and 2.0 min and finally collected on a 10-µm mesh sieve, having been centrifuged between each step. Oxidizing reagents were avoided in order to prevent the loss of more fragile and delicate dinoflagellate cysts [Dale, 1976; Marret, 1993]. Marker-grains of *Lycopodium* spores [Stockmarr, 1977] were added prior to sample treatment in order to calculate cyst concentrations based on the dry weight of sediments. Aliquots of residue were mounted between a slide and coverslide in glycerin jelly, and palynomorphs were studied under a light microscope at 1000x of magnification. All microscope slides and residues are stored in the Paleoenvironmental Laboratory, University of Victoria, Canada.

[15] From 258 to 460 dinoflagellate cysts were counted in each sample (Figure 2), averaging ~360 cysts. Identification was made on the basis of published descriptions in accordance with taxonomy given in Lentin and Williams [1993]. The cyst nomenclature conforms to Head [1996],

**Table 1.** Taxonomic Citation of Dinoflagellate Cysts Used in This Study<sup>a</sup>

Cyst Species (Paleontological Name)	Dinoflagellate Thecate Name or Affinity (Biological Name)
<i>Brigantedinium cariacense</i>	<i>Alexandrium tamarense</i>
<i>Brigantedinium simplex</i>	<i>Protoperidinium avellanum</i>
<i>Brigantedinium</i> spp.	<i>Protoperidinium conicoides</i>
<i>Dubridinium</i> spp.	? <i>Protoperidinium</i> spp.
<i>Echinidinium aculeatum</i>	Diplopsalid group
<i>Echinidinium granulatum</i>	Diplopsalid or Protoperidinoid group
<i>Echinidinium</i> spp.	Diplopsalid or Protoperidinoid group
<i>Impagidinium aculeatum</i>	<i>Gymnodinium</i> spp.
<i>Impagidinium pallidum</i>	<i>Gonyaulax</i> sp. indet.
<i>Impagidinium paradoxum</i>	<i>Gonyaulax</i> sp. indet.
<i>Islandinium brevispinosum</i>	<i>Gonyaulax</i> sp. indet.
<i>Islandinium minutum</i>	<i>Protoperidinium</i> sp. indet.
<i>Islandinium?</i> <i>cezare</i>	<i>Protoperidinium</i> sp. indet.
<i>Lejeunecysta oliva</i>	<i>Protoperidinium</i> sp. indet.
<i>Lingulodinium machaerophorum</i>	<i>Lingulodinium polyedrum</i>
<i>Nematospaeropsis labyrinthus</i>	<i>Gonyaulax spinifera</i> complex
<i>Operculodinium centrocarpum</i> sensu [Wall and Dale, 1966]	<i>Protoceratium reticulatum</i>
<i>Pyxidinopsis reticulata</i>	<i>Pentapharsodinium dalei</i>
<i>Protoperidinium</i> type	<i>Polykrikos kofoidii</i>
<i>Quinquecuspis concreta</i>	<i>Polykrikos schwartzii</i>
<i>Selenopemphix nephroides</i>	<i>Protoperidinium americanum</i>
<i>Selenopemphix quanta</i>	<i>Gonyaulacaceae</i> undif.
<i>Spiniferites bulloideus</i>	<i>Protoperidinium</i> group
<i>Spiniferites membranaceus</i>	<i>Protoperidinium leonis</i>
<i>Spiniferites mirabilis</i>	<i>Protoperidinium subinermis</i>
<i>Spiniferites ramosus</i>	<i>Protoperidinium conicum</i> ; <i>P. nudum</i>
<i>Spiniferites</i> spp.	<i>Gonyaulax scrippsae</i> , <i>G. spinifera</i> complex
<i>Tectatodinium pellitum</i>	<i>Gonyaulax spinifera</i> complex
<i>Trinovantedinium applanatum</i>	<i>Gonyaulax spinifera</i> complex
<i>Trinovantedinium variabile</i>	<i>Gonyaulax scrippsae</i> , <i>G. spinifera</i> complex
<i>Votadinium calvum</i>	<i>Gonyaulax spinifera</i> complex
<i>Votadinium spinosum</i>	<i>Gonyaulax spinifera</i> complex
Spiny brown	<i>Protoperidinium pentagonum</i>
Cyst type A	<i>Protoperidinium divaricatum</i>
	<i>Protoperidinium oblongum</i>
	<i>Protoperidinium claudicans</i>
	? <i>Protoperidinium</i> group
	? <i>Protoperidinium</i> group

<sup>a</sup>The cal equivalents are taken from Head [1996], Zonneveld [1997], Head et al. [2001], and Pospelova and Head [2002].

Zonneveld [1997], Head et al. [2001], and Pospelova and Head [2002] and is provided in Table 1.

[16] Changes in cyst assemblages over time were analyzed by determining the proportions of cysts of heterotrophic and autotrophic dinoflagellates, species richness, Fisher alpha diversity index, the total cyst concentrations as well as the total cyst fluxes (or cyst accumulation rate). Total dinoflagellate cyst flux (cysts cm<sup>-2</sup> yr<sup>-1</sup>), is the product of the total cyst concentration (cysts g<sup>-1</sup>), the sedimentation rate (cm yr<sup>-1</sup>), and the dry bulk density (g cm<sup>-3</sup>).

**Figure 3.** Stratigraphic distribution of concentrations (shaded area) and estimated fluxes (dashed lines) of pollen grains and spores of pteridophytes, foraminiferal organic linings, dinoflagellate cysts, cysts of autotrophic and heterotrophic dinoflagellates. On the left, the diagram illustrates downhole values of dinoflagellate cysts vs. pollen & spores, autotrophic vs. heterotrophic taxa, cyst species richness (solid line) and the Fisher index (dashed line).

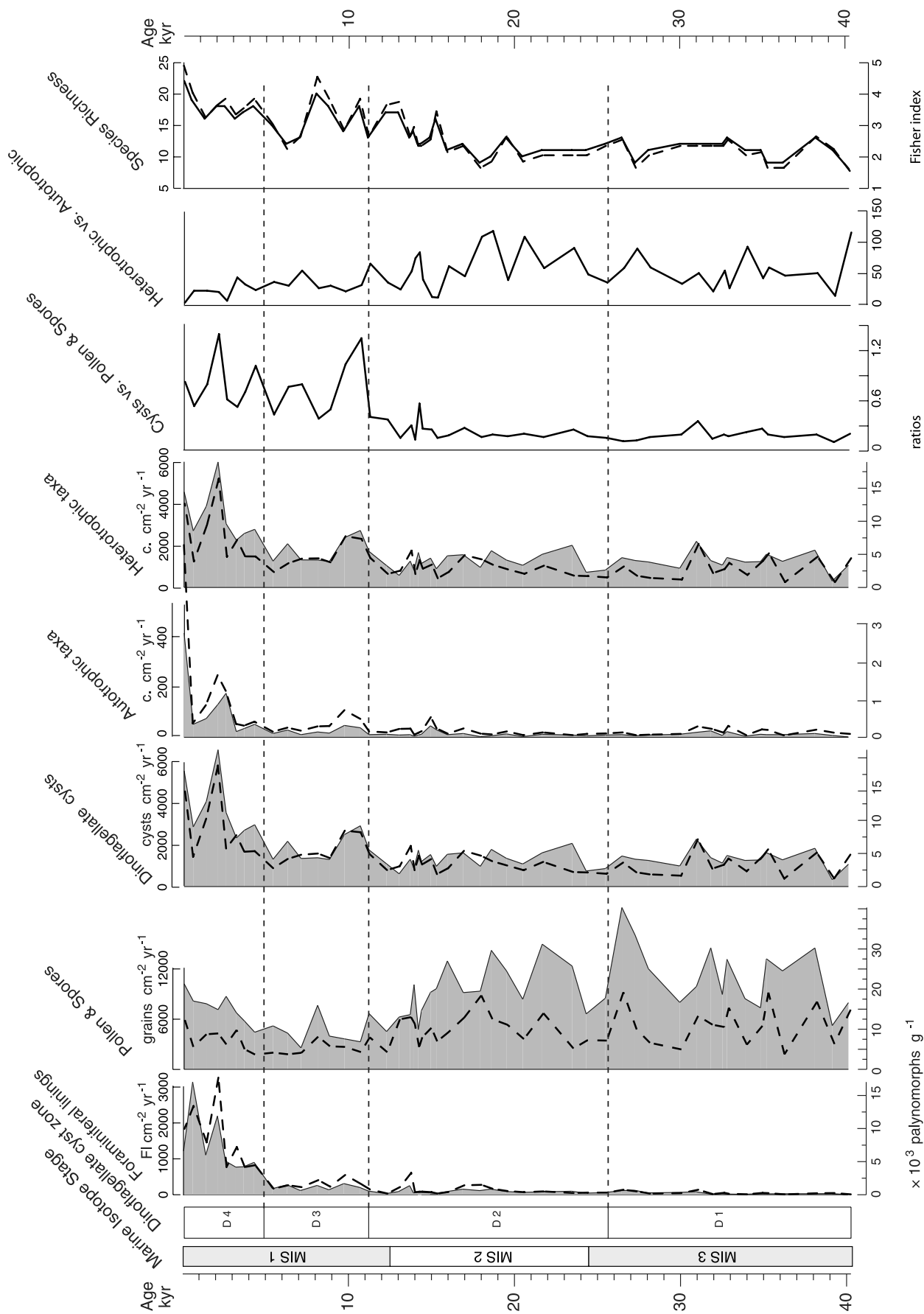


Figure 3

[17] Species richness is used in this study as a measure of dinoflagellate cyst diversity (see discussion in the work of Pospelova et al. [2002, 2005]). In order to make a correction for nonequal cyst counts in samples, the Fisher alpha index, a diversity indicator, was defined for each sample via:

$$S = \alpha * \ln(1 + n/\alpha),$$

where  $S$  is number of cyst taxa (or species richness),  $n$  is the cyst count and  $\alpha$  is the Fisher alpha.

[18] A principal component analysis (PCA) was performed on logarithmic values of relative abundances of dinoflagellate cyst taxa in the assemblages using CANOCO for Windows software. Prior to statistical treatment, some dinoflagellate cyst taxa were grouped together on the basis of morphological similarities. In particular, *Brigantedinium* spp. (*B. cariacense* and *B. simplex*) were grouped together because cyst folding or orientation sometimes obscured the archeopyle characteristics, thus preventing identification to the species level. Because of great morphological similarity between species of the genus *Echinidinium*, all taxa but *E. aculeatum* were grouped as *Echinidinium* spp.

## 4. Results

### 4.1. Palynomorph Concentrations, Fluxes, and Ratios

[19] Core 893A hosts a rich sedimentary record of dinoflagellate cysts, foraminiferal organic linings, pollen grains and spores. Across the sampled sequence, estimated total dinoflagellate cyst concentrations vary by an order of magnitude, from  $\sim 1,000$  to  $20,700$  cysts  $g^{-1}$ , averaging  $\sim 5,700$  cysts  $g^{-1}$  (Figure 3). During the Holocene the total cyst concentrations increased to an average of  $9,100$  cysts  $g^{-1}$  compared with  $4,100$  cysts  $g^{-1}$  in older sediments. This increase is especially pronounced over the last 5 kyr when the total cyst concentrations doubled. Total fluxes of dinoflagellate cysts are calculated to be in  $\sim 300$ – $5,700$  cysts  $cm^{-2} yr^{-1}$  range, with an average of  $1,400$  cysts  $cm^{-2} yr^{-1}$  (Figure 3). As for the total cyst concentrations, a significant increase in the total cyst fluxes occurs in the last 5 kyr.

[20] Throughout the sedimentary sequence cysts produced by heterotrophic dinoflagellates are significantly more abundant than those of autotrophic affinity (Figure 3), averaging  $5,000$  cysts  $g^{-1}$  compared with  $200$  cysts  $g^{-1}$  for autotrophs. Higher total cyst concentrations during the Holocene are due to the increased abundance of cysts produced by heterotrophic taxa. Although relatively low, concentrations of the cysts of autotrophic dinoflagellates increase after the Last Glacial Maximum (LGM), reaching maxima in the second half of the Holocene. This trend is reflected in the heterotrophic to autotrophic cyst ratio (Figure 3), which shows a steady decrease after the LGM.

[21] Total concentrations and fluxes of pollen and spores observed in the core vary from  $\sim 5,400$  to  $40,300$  grains  $g^{-1}$  and from  $1,600$  to  $9,000$  grains  $cm^{-2} yr^{-1}$  (Figure 3). In the pre-Holocene section, the average concentration of pollen and spores is  $\sim 21,000$  grains  $g^{-1}$ , decreasing to  $\sim 12,100$  grains  $g^{-1}$  during the Holocene. This trend is opposite to that of the total dinoflagellate cyst abundance.

[22] The abundance of foraminiferal organic linings increases significantly during the Holocene and particularly over the last 5 kyr (Figure 3). Concentrations change from  $\sim 30$  to  $1,400$  linings  $g^{-1}$  between 40 and 12 kyr to  $\sim 800$  to  $1,700$  linings  $g^{-1}$  between 12 and 5 kyr, but average  $7,500$  linings  $g^{-1}$  during the second half of the Holocene.

### 4.2. Dinoflagellate Cyst Assemblages

[23] Forty cyst taxa were identified in the studied section of the core (Tables 1 and 2). The number of species varies from 9 to 22 (Figure 3), with an average of 13, while the Fisher index changes from 1.6 to 5.0 (Figure 3). There is a general increase in species richness after the LGM, which reaches its maximum during the Holocene.

[24] Throughout the sequence, the dinoflagellate cyst assemblages are dominated by the round brown *Proto-peridinium* cysts, primarily *Brigantedinium* spp. that are accompanied by *Dubridinium* spp., *Echinidinium* spp., *Quinquecuspis concreta*, *Selenopemphix nephroides*, *S. quanta*, and cysts of *Proto-peridinium americanum* (Figure 2 and Figures S1, S2, and S3 in auxiliary material<sup>1</sup>). Cysts of the Gonyaulacales, primarily *Spiniferites ramosus*, *Spiniferites* spp., *Lingulodinium machaerophorum*, and *Operculodinium centrocarpum* sensu Wall & Dale, 1966, rarely contribute more than 2% of the assemblages. Cysts belonging to the order *Gymnodinales*, namely *Polykrikos kofoidii*, are occasionally present at  $<2\%$ .

[25] Principal component analysis (PCA), performed on cyst taxa percentages, yielded two first principal components that represent, respectively, 31 and 17% of the total variance (Figure 2). Ordination of each taxon based on the two first principal component axes is shown in Figure 4. All the autotrophic taxa are ordinated on the positive side of the first principal component axis (PC1), whereas most heterotrophic taxa are scattered and form several groups (Figure 4). The group of heterotrophic-related *Polykrikos kofoidii*, *Proto-peridinium americanum*, *Echinidinium aculeatum*, *Islandinium minutum*, and spiny brown cysts have positive PC1 values, whereas *Brigantedinium* spp. and *Selenopemphix nephroides* have negative values. From an ecological perspective, taxa in the first group tend to indicate warmer nutrient-rich waters, while the second group indicates cooler nutrient-rich environments. This suggests that PC-1 reflects the temperature gradients in nutrient-rich environments, with higher values implying warmer waters. As seen in Figure 5, PC-1 exhibits a clear trend over the temporal scales of several kyr, having its maximal values during the Holocene, steadily decreasing to the LGM, and having its intermediate values during Marine Isotopic Stage 3 (MIS). It remains to be seen whether smaller amplitude variations of PC-1 on millennial to submillennial scales could be interpreted as temperature fluctuations.

[26] Four dinoflagellate cyst zones (D1–D4) were recognized, based primarily on the results of the PCA and the relative abundance of individual dinoflagellate cyst taxa (Figure 2).

<sup>1</sup>Auxiliary material is available at <ftp://ftp.agu.org/apend/pa/2005pa001251>.

**Table 2.** Estimated Fluxes or Accumulation Rates of Palynomorphs Including Those of Dinoflagellate Cysts, Total Pollen and Spores, and Foraminiferal Organic Linings in Hole 893A<sup>a</sup>

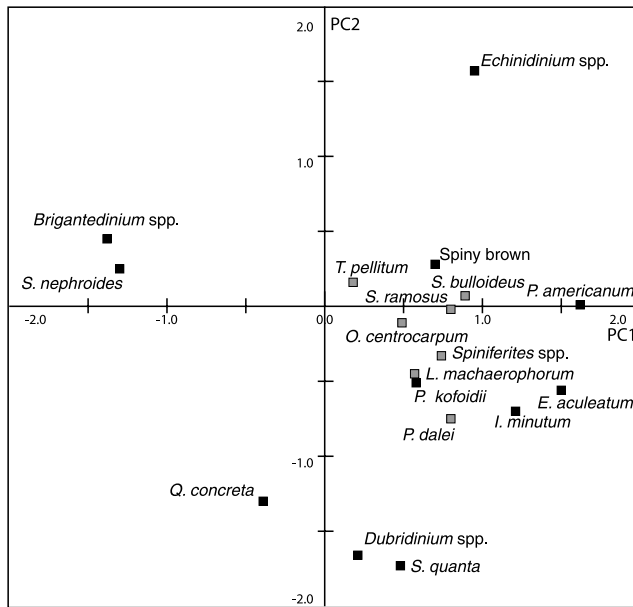
Leg	Hole	Core	Int min, cm	Int max, cm	RB Depth, mbsfm	Age, kyr	Total Pollen and Spores Flux	Total Dinoflagellate Cyst Flux	Autotrophic Cysts	Heterotrophic Cysts	<i>Alexandrium tamariscense</i>	<i>Impagidinium spp.</i>	<i>Impagidinium aculeatum</i>	<i>Impagidinium pallidum</i>	<i>Impagidinium paradoxum</i>	<i>Lingulodinium machaerophorum</i>	<i>Nematospaeroopsis labyrinthus</i>	<i>Operculodinium centrocarpum sensu Wall and Dale, 1966</i>
1	146	893A	1H-1	3	4	0.03	5912	4849	786	4003	12	24	0	0	0	339	0	48
2	146	893A	1H-1	107	108	1.07	2472	1309	53	6	6	0	3	0	0	9	0	6
3	146	893A	1H-2	96	97	2.46	3980	3130	126	3130	0	8	0	0	0	0	0	0
4	146	893A	1H-3	64	65	3.65	4080	5666	246	5198	0	12	0	0	0	0	0	0
5	146	893A	1H-3	146	147	4.47	2772	1702	183	1467	0	4	0	0	0	0	0	17
6	146	893A	1H-4	95	96	5.46	4487	2338	51	2275	0	0	0	0	0	0	0	13
7	146	893A	1H-5	26	27	6.25	2198	1548	44	1486	0	0	4	0	0	0	0	15
8	146	893A	2H-1	75	76	7.28	432	1577	60	1481	0	0	0	8	0	0	0	13
9	146	893A	2H-2	86	87	8.91	535	1786	761	735	0	0	0	0	2	0	0	24
10	146	893A	2H-3	96	97	10.48	635	1589	36	1162	0	0	0	0	0	0	0	8
11	146	893A	2H-4	85	86	11.66	1769	1405	24	1380	0	0	0	0	0	0	0	12
12	146	893A	2H-5	116	117	13.38	823	3874	49	1392	0	4	0	4	0	0	0	8
13	146	893A	2H-6	86	87	14.39	889	1249	38	1202	0	0	0	0	0	0	3	13
14	146	893A	2H-7	75	77	15.71	975	2471	106	2450	0	7	0	0	0	0	0	21
15	146	893A	3H-1	115	116	17.14	1070	1853	71	2322	0	0	0	0	0	0	0	19
16	146	893A	3H-2	45	46	17.89	1118	1440	21	1415	0	0	4	0	0	0	0	8
17	146	893A	3H-3	55	56	19.47	1224	1836	17	648	0	2	0	0	0	0	0	2
18	146	893A	3H-4	25	26	20.64	5766	853	31	806	0	3	0	0	0	3	0	0
19	146	893A	3H-4	126	127	21.65	1370	6024	32	1761	0	0	11	0	0	0	0	0
20	146	893A	3H-5	15	16	21.99	1392	5216	8	641	0	0	0	0	0	0	0	2
21	146	893A	3H-5	56	57	22.4	1400	2443	16	1306	0	0	0	0	0	0	0	0
22	146	893A	3H-5	95	96	22.79	1446	3622	939	898	0	0	0	0	3	0	0	5
23	146	893A	3H-6	28	29	23.48	1493	4743	1196	1095	0	0	0	0	0	0	0	23
24	146	893A	3H-6	85	86	24.05	1531	3136	33	440	0	0	0	0	0	0	3	4
25	146	893A	3H-7	35	36	24.96	1592	761	12	746	0	0	0	0	0	0	0	2
26	146	893A	4H-1	115	116	26.95	1727	5968	33	1545	0	0	0	0	0	5	0	0
27	146	893A	4H-2	124	125	28.33	1821	1357	12	1341	0	0	0	0	0	0	0	0
28	146	893A	4H-3	75	76	29.27	1885	5783	9	1084	0	0	0	0	0	0	0	0
29	146	893A	4H-4	70	71	30.66	1908	5112	21	862	0	0	0	0	0	0	0	8
30	146	893A	4H-5	94	95	32.19	2085	3405	6	655	0	0	0	0	0	0	0	0
31	146	893A	4H-6	126	127	33.91	2203	6488	17	1043	0	0	0	0	0	0	0	3
32	146	893A	5H-1	116	117	36.24	2364	2282	6	565	0	0	0	0	0	0	0	2
33	146	893A	5H-2	102	103	37.5	2451	3276	11	544	0	2	0	0	0	0	0	2
34	146	893A	5H-3	135	136	39.21	2569	3225	13	479	0	0	0	0	0	0	0	3
35	146	893A	5H-5	16	17	40.84	2683	8986	17	1005	0	0	0	0	0	8	3	0
36	146	893A	5H-5	115	116	41.83	2751	4566	6	558	0	0	0	0	0	0	0	0
37	146	893A	5H-6	105	106	43.21	2848	2961	8	455	0	0	0	0	0	0	0	3
38	146	893A	6H-1	85	86	45.19	3004	2168	11	379	0	0	0	0	0	0	0	0
39	146	893A	6H-2	95	96	46.5	3072	6169	41	2086	0	0	0	0	0	0	0	6
40	146	893A	6H-3	65	66	47.56	3193	5117	31	687	0	0	0	0	0	0	0	8
41	146	893A	6H-4	16	17	48.44	3263	4849	16	882	0	3	0	0	0	0	0	5
42	146	893A	6H-4	55	56	48.83	3294	7130	43	1175	0	0	0	0	3	0	0	21
43	146	893A	6H-5	45	46	50.21	3405	2748	6	598	0	0	0	0	0	0	0	5
44	146	893A	6H-6	15	16	51.37	3497	4984	29	1270	0	4	0	0	0	0	0	22
45	146	893A	6H-6	65	66	51.87	3537	8954	167	1633	0	0	0	0	0	0	0	13
46	146	893A	6H-7	45	46	53.13	3638	1595	5	257	0	0	0	0	0	0	0	4
47	146	893A	7H-3	45	46	55.46	3802	7862	28	1467	0	0	0	0	0	0	0	0
48	146	893A	7H-4	75	76	57.02	3927	2833	16	253	0	1	0	0	0	0	0	1
49	146	893A	7H-5	45	46	58.03	4008	6915	11	1401	0	0	0	0	0	0	0	4



Table 2. (continued)

<i>Voadinium spinosum</i>	Cyst of <i>Protopertidium americanum</i>	<i>Quinquecuspis concreta</i>	Cyst of <i>Polytrikos schwartzii</i>	Cyst of <i>Polytrikos kofoidii</i>	<i>Dubridinium spp.</i>	<i>Echinidinium aculeatum</i>	<i>Echinidinium concretum</i>	<i>Echinidinium spp.</i>	Spiny Brown	Unknown Cysts	Fossiliferous Organic Linings	<i>Heterosigma akashiwo</i>	<i>Halodinium spp.</i>	<i>Pediastrum spp.</i>	<i>Hexasterias problematica</i>	<i>Radiosperma corbiferum</i>	Mandibles
0	218	60	0	60	85	85	97	36	24	1835	12	24	0	0	0	0	36
0	103	19	0	0	12	19	81	12	0	2472	25	12	0	0	12	0	31
0	204	8	0	0	24	31	165	8	8	1459	8	8	0	0	3	8	79
12	259	135	0	37	49	185	259	172	49	3264	0	37	0	0	16	8	74
0	104	22	0	4	22	39	100	39	13	774	9	4	0	0	37	0	13
6	184	51	0	25	57	6	178	6	6	1330	0	19	0	0	0	0	38
0	151	11	0	7	29	18	177	4	15	771	4	7	4	0	6	0	29
8	60	24	0	4	76	28	331	12	24	824	8	0	4	0	0	4	48
0	16	4	0	4	30	6	30	6	0	170	0	0	4	0	0	0	28
0	12	0	0	0	48	9	36	0	6	265	3	0	0	0	0	0	15
0	4	20	0	0	98	4	24	0	0	212	0	12	4	0	0	0	29
8	8	4	0	8	119	25	54	12	8	474	4	4	0	0	0	0	29
0	0	16	0	3	63	9	44	3	6	230	0	3	0	0	3	0	22
0	7	0	0	0	219	21	85	0	0	551	7	0	0	0	0	0	56
0	6	21	0	0	19	19	58	65	19	298	13	0	0	0	0	0	13
0	0	136	0	0	106	4	42	0	4	149	0	8	0	0	0	0	42
0	0	13	0	0	19	0	8	0	6	33	2	6	0	0	0	0	12
0	0	19	0	4	8	0	16	8	8	215	5	3	0	0	0	0	21
0	0	16	0	0	22	13	16	16	16	608	0	5	0	0	0	0	27
0	0	81	0	11	4	2	27	6	8	70	0	4	0	0	0	0	21
0	0	17	0	0	4	0	21	12	0	85	0	4	0	0	0	0	16
0	0	27	0	4	31	2	23	12	23	87	0	0	0	0	0	0	16
0	0	27	0	0	14	3	11	0	19	87	0	3	0	0	0	0	14
7	0	68	0	0	16	0	59	0	23	72	0	0	0	0	0	0	7
0	0	28	1	9	22	0	9	1	3	33	0	0	1	0	0	0	10
0	0	26	0	0	21	0	5	0	2	76	0	2	0	0	0	0	36
0	0	0	0	5	38	0	38	0	14	264	0	0	0	0	0	0	99
0	0	33	0	8	37	0	0	0	0	276	0	0	0	0	0	0	65
3	0	8	0	0	0	0	0	0	4	276	0	0	0	0	0	0	65
0	0	21	0	0	15	0	9	0	3	167	0	0	0	0	0	0	40
0	0	24	0	3	26	0	13	3	3	102	0	5	3	0	0	0	13
0	0	18	0	0	8	0	0	4	2	72	0	0	0	0	0	0	22
0	0	32	0	0	78	0	17	0	0	93	0	0	0	0	0	0	20
0	0	9	0	0	12	0	31	3	5	48	0	0	0	0	0	0	11
0	0	9	0	0	11	0	11	2	3	59	0	0	0	0	0	0	11
0	0	7	0	0	10	0	17	3	1	59	0	1	0	0	0	0	14
0	0	17	0	3	8	0	62	6	3	140	0	0	0	0	0	0	53
0	0	2	0	5	2	0	23	2	0	93	0	0	0	0	0	0	23
0	0	1	0	0	4	0	40	4	0	34	0	0	0	0	0	0	13
0	0	2	1	0	9	0	65	11	4	46	0	0	0	0	0	0	4
0	0	23	0	6	6	0	52	12	6	139	0	0	0	0	0	0	4
0	0	10	0	0	4	0	85	17	4	19	0	2	0	0	0	0	12
0	0	27	0	5	8	0	16	16	11	54	0	0	3	0	0	0	14
0	0	24	0	0	9	0	55	6	0	27	0	0	0	0	0	0	16
0	0	5	0	2	0	0	60	8	3	13	0	0	0	0	0	0	24
0	0	11	0	0	15	0	29	0	7	51	0	0	0	0	0	0	16
0	0	18	0	0	4	0	36	0	4	45	0	0	4	0	0	0	4
0	0	2	0	0	1	0	13	0	1	10	0	0	0	0	0	0	4
0	0	5	5	0	0	0	163	0	9	42	0	0	0	0	0	0	2
0	0	3	0	0	4	0	20	0	2	47	1	3	0	0	0	0	5
0	0	25	0	4	7	0	50	0	0	11	0	7	0	0	0	0	1

<sup>a</sup>Palynomorphs in cm<sup>-2</sup> yr<sup>-1</sup>.



**Figure 4.** Ordination of dinoflagellate cyst taxa based on the results of the Principal Component Analysis. The first PC axis represents 32% of the variance and the second 18%. The black and gray squares identify cysts of heterotrophic and autotrophic taxa, respectively.

#### 4.2.1. Zone D1 (Samples From 40.08 to 26.83 kyr)

[27] The cyst assemblages in this zone are marked by the highest number of *Brigantedinium* spp. (~84.7%), relatively high abundance of *Echinidinium* spp. (~6.4%), and a constant presence of *Selenopemphix nephroides* (~2.4%). Cysts produced by autotrophic taxa contribute to less than 2.5% of the assemblages. This zone is characterized by negative PC1 and the highest positive PC2 values and approximately corresponds to the upper section of MIS 3.

#### 4.2.2. Zone D2 (Samples From 25.69 to 11.18 kyr)

[28] Relative abundances of *Selenopemphix nephroides* (~3.6%) and *Quinquecuspis concreta* (~2.6%) increase noticeably in dinoflagellate cyst zone D2. *S. nephroides* reaches its maximum (9.1%) during the LGM, whereas *Echinidinium* spp. declines and exhibits the lowest values. *Brigantedinium* spp. and *Dubridinium* spp. comprise ~82.7 and 2.6% of the assemblages, respectively. Autotrophic-related taxa contribute to less than 2.5% of the cyst assemblages. Zone D2 is generally characterized by the lowest negative PC1 and PC2 values. This zone can be roughly matched to MIS 2, which includes the LGM.

#### 4.2.3. Zone D3 (Samples From 10.70 to 5.35 kyr)

[29] The zone is marked by an increase of *Dubridinium* spp. (~6.9%), appearance of cysts of *Protoperidinium americanum* (~0.6%), relative rise in the abundance of *Echinidinium* spp., and decrease of *Selenopemphix nephroides* (~1.1%) and *Quinquecuspis concreta* (~1.4%), as well as a constant presence of *Echinidinium aculeatum* (0.8%). *Brigantedinium* spp. dominates assemblages at ~79.2%. Cysts of autotrophic dinoflagellates comprise ~3% of the assemblages. Zone D3 is characterized by positive PC1 and negative PC2 values, and approximately

corresponds to the first half of MIS 1 or the first part of the Holocene.

#### 4.2.4. Zone D4 (Samples From 4.32 to 0.01 kyr)

[30] An abrupt increase in *Echinidinium* spp. (up to 21% or less) and cysts of *Protoperidinium americanum* (~6.4%) characterize this zone. *Dubridinium* spp. gradually diminishes, averaging ~1.8%. The zone is also marked by the lowest abundance of *Selenopemphix nephroides* (~0.6%) and *Brigantedinium* spp. (67.6%), whereas cysts of autotrophic dinoflagellates increase to ~6%, primarily due to *Spiniferites* and *Lingulodinium machaerophorum* in the top samples. Zone D4 has the highest PC1 values and frequent fluctuations of PC2. This zone corresponds to the second half of MIS 1 or the most recent part of the Holocene.

### 4.3. Reconstructions of Sea-Surface Conditions With the Best Analog Technique

[31] A reconstruction of the sea-surface conditions based on the best analogue technique was attempted for this core. Dinoflagellate cyst assemblages from the core samples were matched to the existing reference database that includes 1054 sites from the North Atlantic and Northeastern Pacific [de Vernal et al., 2001, 2005]. We followed the procedure described by de Vernal et al. [2001]. The minimal mean distance of the closest modern analog from the reference assemblages and the core assemblages were very high (>50), and beyond the threshold values for reliable reconstruction. Significant number of dinoflagellate cyst assemblages from Core 893A had no analogs in the existing database. The absence of analogs and/or large dissimilarity values can be partially explained by the low number of the surface samples from this part of the Pacific, and upwelling zones in particular.

## 5. Discussion

### 5.1. Major Changes in Climate and Paleoproductivity in the Cyst Record

[32] Dinoflagellate cyst accumulation rates are considered to reflect export production [Dale, 1996; Reichart and Brinkhuis, 2003]. The rates observed in this work are extremely high, being on average approximately two orders of magnitude higher than fluxes reported from the Gulf of Alaska [de Vernal and Pedersen, 1997], but similar to those reported in Arabian Sea sediments [Zonneveld and Brummer, 2000; Reichart and Brinkhuis, 2003]. Such high accumulation rates, on the order of  $10^3$  cysts  $\text{cm}^{-2} \text{yr}^{-1}$ , are characteristic of active upwelling regions.

[33] The temporal trends seen in both total cyst concentrations and fluxes in Core 893A, in particular the twofold increase in both parameters during the Holocene (Figure 3), coincide with higher concentrations of organic carbon seen in previous work (Figure 5), supporting the notion that cyst burial fluxes are a proxy for export production. We find a significant linear correlation between the total dinoflagellate cyst concentrations and %TOC shown in Figure 6, reflecting covariant changes in these proxies of paleoproductivity.

[34] Another evidence for the variation in the paleoproductivity over the last 40 kyr in the Santa Barbara Basin is the change in the ratio of total cyst concentration to the total concentration of pollen and spores. This ratio can be used as

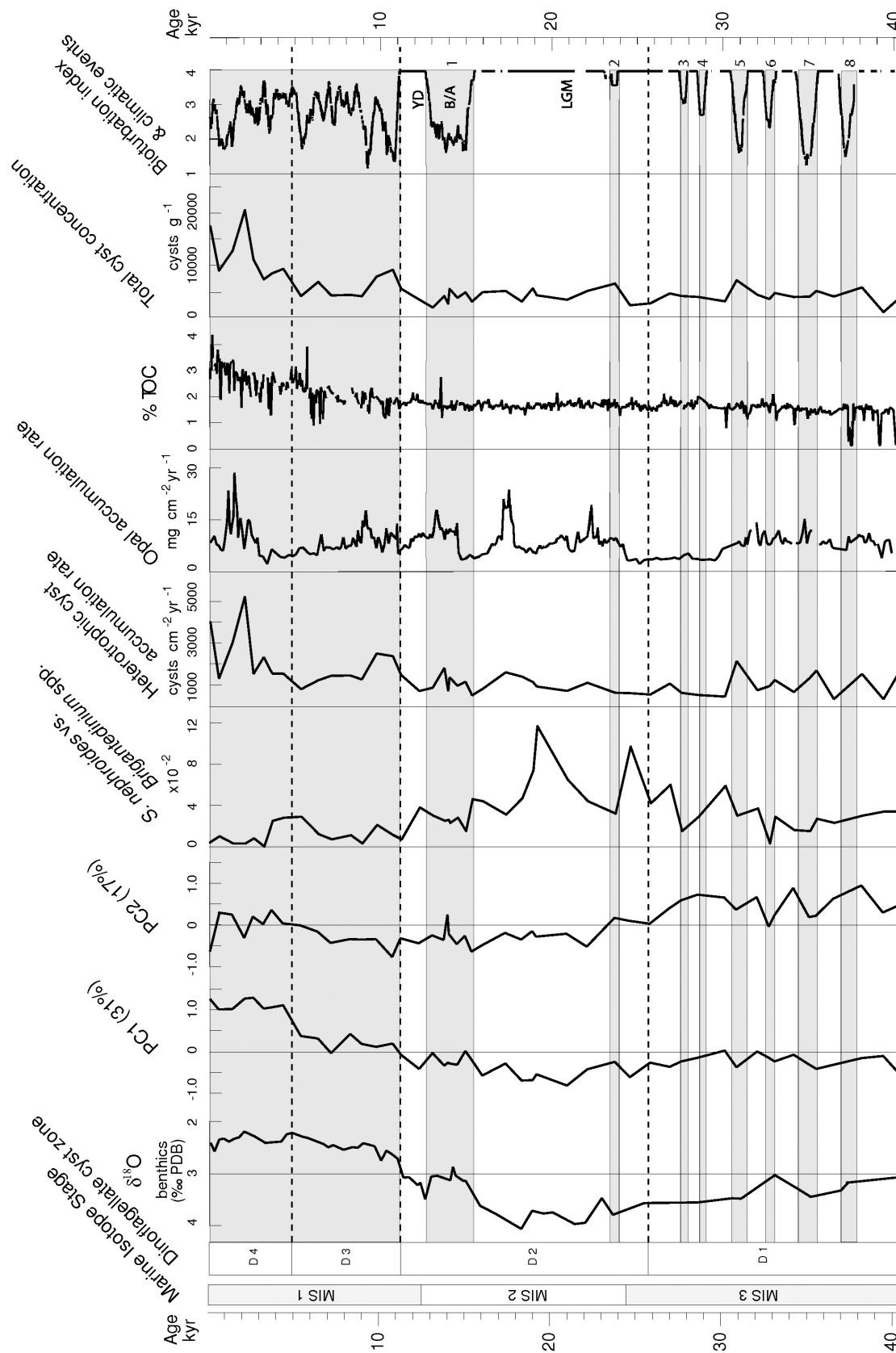


**Figure 5.** A comparison of bioturbation index (1 indicates massive bioturbated sediment facies) [Behl and Kennett, 1996], records of benthic  $\delta^{18}\text{O}$  [Behl and Kennett, 1996], %TOC [Gardner and Darnell, 1995; Stein and Rack, 1995; Ivanochko and Pedersen, 2004], and opal accumulation rate [Ivanochko and Pedersen, 2004] with values of PC1 and PC2 in Hole 893A. Gray bands represent warm climatic events (interstadials and the Holocene). Interstadials are numbered in accordance with GISP2.

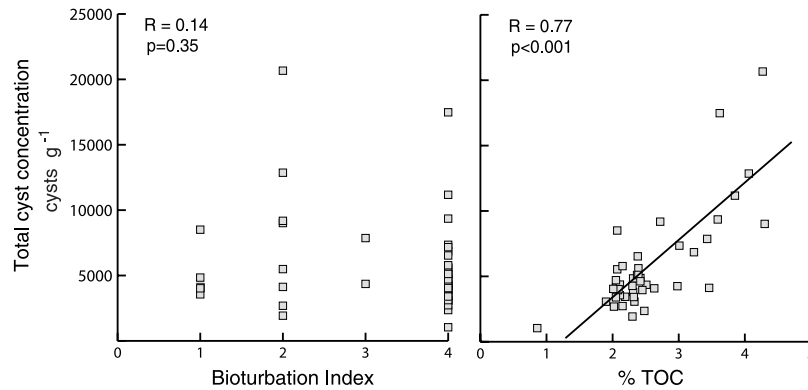


**Figure 6.** Correlation of total dinoflagellate cyst concentrations with bioturbation index and %TOC.

a proxy for comparison of marine and terrestrial productivities. The ratio of total cyst concentration to the total concentration of pollen and spores shows a substantial change in the Holocene (Figure 3), increasing from 0.2 in the pre-Holocene to 0.8 during the Holocene, reflecting an increase in marine production relative to terrestrial input during this period. The increase in marine production during the Holocene, and its second part in particular, is also evident from the substantial increase in the concentrations and fluxes of foraminiferal organic linings (Figure 3).

[35] High abundances of cysts produced by heterotrophic dinoflagellates in upwelling regions have been previously reported [Lewis *et al.*, 1990]. Our results, showing the dominance of *Protoperidinium* in the cyst assemblages, and *Brigantedinium* spp. in particular, agree with such observations. Since the cysts of *Protoperidinium* contribute >60% of the dinoflagellate cyst populations throughout the sequence, and given the association of this group of organisms with upwelling zones, we conclude that coastal upwelling continued to influence Santa Barbara Basin over the late Quaternary, albeit with some degree of waxing and waning.

[36] The distribution of heterotrophic dinoflagellates reflects the availability of their preferable prey, diatoms and small flagellates. Both are typically highly abundant in upwelling regions [Taylor, 1987]. Hence it is logical to expect a correlation between cyst abundance and diatomaceous opal accumulation, and such a relationship is indeed observed (Figure 5).

[37] The relatively low concentrations of cysts produced by autotrophic dinoflagellates throughout MIS 3 and MIS 2 suggest that the contribution of dinoflagellates to primary production was limited in these intervals, while the increased concentrations and fluxes of such cysts in the post-LGM deposits imply a more substantial contribution, particularly in the late Holocene.

[38] The increase in the abundances of cysts produced by autotrophic dinoflagellates, *Spiniferites* group and *Lingulodinium machaerophorum* in particular, over the latest part of the Holocene could signal the enhanced input of warm and nutrient rich waters from the south. This conclusion is instigated by the observation of a substantial increase of

relative abundance of cysts produced by autotrophic dinoflagellates southward from Point Conception [Pospelova, 2005]. Other studies of dinoflagellate cysts records over the last 200 yr in the SBB find that the proportion of *Spiniferites* has a positive correlation with temperature [Prauss, 2002]. We believe that in Core 893A the ratio of heterotrophs to autotrophs can be used as a proxy for paleotemperature: the lower ratio would correspond to warmer waters.

[39] Changes in the composition of dinoflagellate cyst assemblages indicate SST variability in the Santa Barbara Basin reflected in the change of PCA1 values. Dinoflagellate cyst assemblages (zone D2) from MIS 2, and particularly the LGM, have the lowest score for PCA1 and are characterized by the increase of cysts of heterotrophic dinoflagellates, in particularly *Selenopemphix nephroides*. Present day distribution of *Selenopemphix nephroides* along the Pacific coast of North America shows that similar abundances (5–10%) are found in surface sediments off the coast of Oregon (40–45°N), decreasing southward [Radi and de Vernal, 2004; Pospelova, 2005]. *Selenopemphix nephroides* is commonly found in the association with *Brigantedinium* spp. in this region, but the latter exhibits apparently a much wider latitudinal distribution and likely has a larger temperature tolerance range. Therefore we suggest that the increase in the ratio of abundances of *Selenopemphix nephroides* and *Brigantedinium* spp. in the SBB core may be used as a qualitative signal of cooling episodes in the SBB. The ratio (Figure 5) peaks at the LGM indicating the decrease in SST. This suggests a substantial cooling of sea-surface waters in the Santa Barbara Basin during the LGM possibly caused by migration of cold subarctic waters to the region. A rough estimate for the SST during the LGM can be drawn from the comparison of present-day SST off the coast of Oregon with that in the SBB. An average August SST [Radi and de Vernal, 2004; Pospelova, 2005] off the coast of Oregon is ~11–12°C, which is 5–6°C lower than the present-day SST in the Santa Barbara Basin. This suggests a similar, 5–6°C, difference in the SST between the LGM and the present. These values agree with the change in SST inferred from the foraminiferal assemblages [Hendy and Kennett, 2000] and are some-

**Table 3.** Summary of Average Values for Main Parameters of Dinoflagellate Cyst Record in Hole 893A

Marine Isotope Stage	MIS3	MIS2	LGM (22–16 kyr)	MIS1
Dinoflagellate cyst zone	D1	D2	D2	D3 and D4
PC1	−0.23	−0.4	−0.58	0.59
Flux of heterotrophic dinoflagellate cysts (cysts cm <sup>−2</sup> yr <sup>−1</sup> )	912	958	1,039	1,932
Flux of autotrophic dinoflagellate cysts (cysts cm <sup>−2</sup> yr <sup>−1</sup> )	19	22	16	114
Ratio of heterotrophs to autotrophs	55	63	79	31
Ratio of <i>Selenopemphix nephroides</i> to <i>Brigantedinium</i> spp.	0.03	0.05	0.06	0.01
Species richness/Fisher index	11/2.2	12/2.5	11/2.1	17/3.6

what larger than 2–3°C temperature difference between the LGM and the present-day values suggested by the alkenone paleotemperature analysis [Herbert *et al.*, 1995].

[40] We summarized the average values for the main parameters of the dinoflagellate cyst assemblages for the following intervals: MIS 3, MIS 2 (including the LGM), the LGM, and MIS 1 in Table 3. Changes of paleotemperatures are reflected in values of PC1, the ratio of heterotrophs to autotrophs, and the ratio of *Selenopemphix nephroides* to *Brigantedinium* spp., whereas the dinoflagellate cyst production is signaled by the fluxes of heterotrophic dinoflagellate cysts. Indeed, MIS 1 (the Holocene) and the LGM are set apart by all parameters. Comparing characteristics of dinoflagellate cyst records during MIS 3 with those of the LGM and the Holocene, we find that most of the parameters in MIS 3 have intermediate values, suggesting that on average the SST during MIS 3 were lower than those in the Holocene but higher than during the LGM. At the same time, there is no evidence that the marine productivity during MIS 3 was higher than in the LGM.

## 5.2. Climatic Events During MIS 2 and 3

[41] The ~1 kyr sampling frequency in MIS 2 and MIS 3, and ~500 yr sampling in the interval from 15 to 10 kyr allows identification of a number of climatic events in the dinoflagellate cyst record.

[42] Prior to the Holocene the paleoproductivity, estimated using the total concentrations and fluxes of dinoflagellate cysts, remains relatively stable throughout the sequence. However, during the studied upper section of MIS 3 the total cyst fluxes experience significant modulation, showing a factor of 7–10 contrast between the minima and maxima (Figures 3 and 5). This modulation can be distinctly seen in the fluxes of cysts of heterotrophic, autotrophic dinoflagellates and foraminiferal organic linings (Figure 7). Maxima in cyst fluxes coincide, within our accuracy, with warm events in MIS 3 (Figure 7). In particular, warm Dansgaard-Oeschger events 8, 7, 6, and 5 are associated with increased total cyst and foraminiferal organic lining accumulation rates (Figure 7). Both imply higher export production during the events. A more detailed sampling would be needed in order to establish a more precise correspondence between the increases in the dinoflagellate production and the D-O events. This might also help in detecting eventual SST changes, notably the interstadial events 2, 3 and 4 that are characterized by a short duration.

[43] More detailed sampling of the 10–15 kyr interval defines decreased cyst accumulation (thus implied production) during the Younger Dryas episode, and increased

accumulation (thus high export productivity) during warm Bolling-Allerod (Figure 7). A drop in the productivity is also seen during an episode associated with the Older Dryas. The Bolling is also marked by a large increase in fluxes of cysts of autotrophic dinoflagellates, and an increase in the relative abundance of *Spiniferites* spp. which is associated with warmer conditions. During the LGM, an increase in marine productivity can be seen at 19–17 kyr (Figure 7).

[44] Quantitative reconstruction of the paleotemperature oscillations between stadials and interstadials during the MIS 3 were attempted in the work of Hendy and Kennett [1999] with the use of the foraminiferal record. Reconstruction of SST based on stable isotopic analysis suggested rather large, ~5 to 6°C, amplitude of variation in the SST between stadial and interstadial episodes of the MIS 3. Methods based on species composition of foraminiferal assemblages, the transfer function and modern analogue techniques, suggested similar amplitude of the SST modulation, yet displaying a systematic shift of few degrees to lower temperatures [Hendy and Kennett, 2000]. Noticeably, this conclusion differs from the alkenone determinations of the paleotemperature in the SBB [Herbert *et al.*, 1995; Doose *et al.*, 1997], which suggest a reduced range of the SST change between stadials and interstadials of 1 to 2°C. Dinoflagellate cyst record provides some indirect support to the interpretation of a reduced SST variation between stadials and interstadials during the MIS 3. Although these events are easily seen in the total cyst fluxes and concentrations, the composition of cyst taxa does not show substantial millennial-scale variations, which implies either the absence of strong changes in the SST or a reduced response of dinoflagellates to the high-frequency climate variations. The latter option seems to be unlikely given the 1–2° sensitivity of the dinoflagellate cyst assemblages to the changes of the SST seen in the modern records.

## 5.3. Cyst Preservation

[45] The variations in dinoflagellate cyst fluxes observed between stadials and interstadials raises the issue as to whether this is a genuine signal of changing export production or an artifact of poor cyst preservation resulting from well-oxidized conditions in the surface sediments during the stadials. Three lines of evidence argue against the latter possibility. First, we did not detect any visual cyst degradation during stadials relative to interstadials, and the preservation of cysts of all taxa was very good throughout the entire sedimentary sequence. Second, if postdepositional oxidation had caused cyst degradation in the core, one could

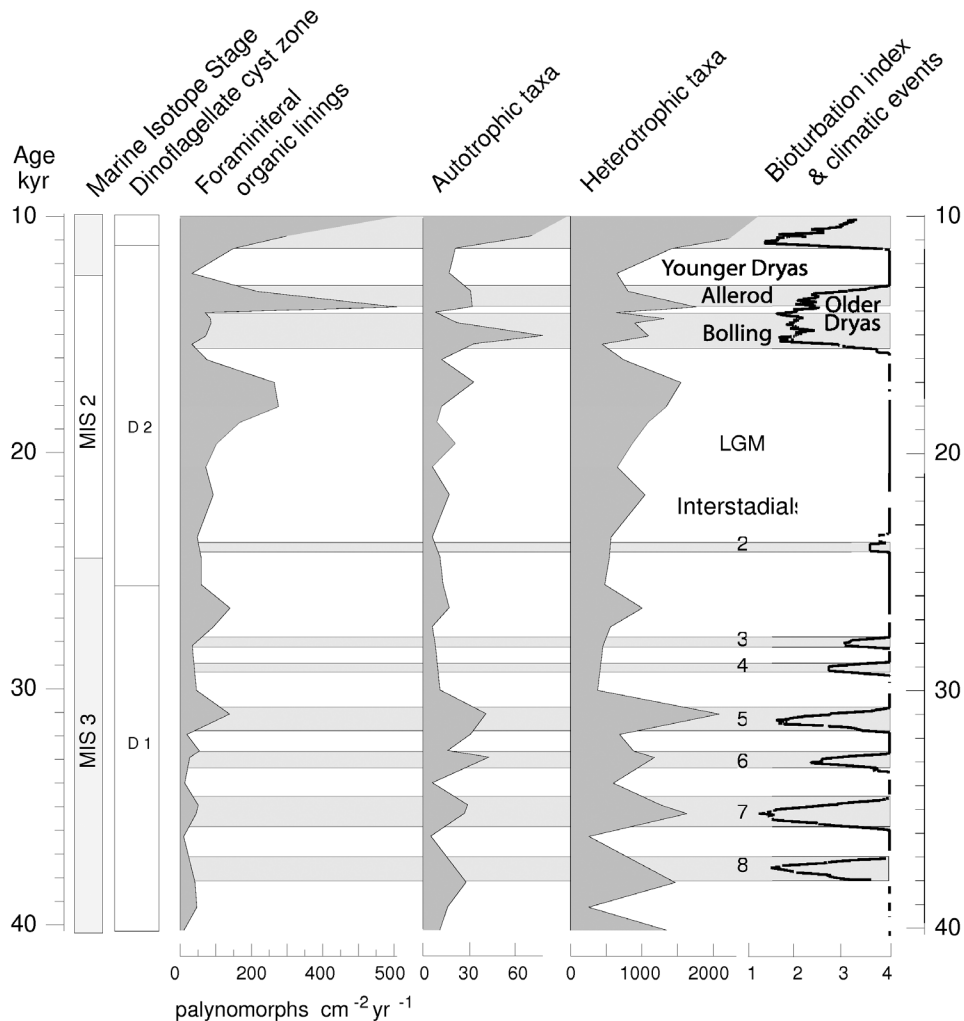


**Figure 7.** Flux estimates of foraminiferal organic linings and cysts of heterotrophic and autotrophic dinoflagellates for 40–10 kyr. Gray bands represent warm climatic events (interstadials and the Holocene).

expect a significant negative correlation to exist down core between the bioturbation index and the total cyst fluxes and/or concentrations. No such correlation is seen (Figure 6). Third, if oxidation had modulated cyst burial fluxes during MIS 3 to the degree observed (i.e. suppressing the apparent cyst fluxes by a factor of 7–10 during stadials), the same suppression should have applied to the LGM, when bottom sediments were also well oxidized. This would lead to a dramatic conclusion that the actual productivity during the LGM had been almost an order of magnitude higher than indicated by the supposed “oxidized” assemblage. Such a conclusion is not corroborated by any other proxy of productivity [see, e.g., *Ivanochko and Pedersen, 2004*]. Therefore we conclude that the influence of oxidation on cyst preservation in the SBB during the late Quaternary was minimal.

## 6. Conclusions

[46] This work presents the first investigation of the late Quaternary history of dinoflagellate cyst accumulation in

the Santa Barbara Basin. Dinoflagellate cysts are abundant throughout the studied section of Core 893A, which spans some 40,000 years, and accumulated at rates comparable to those observed in other upwelling regions around the world. Assemblages are dominated by *Brigantedinium* spp., implying that upwelling was continuously present in the region during the last 40 kyr. The Holocene and the Last Glacial Maximum are clearly identifiable on the basis of cyst abundance, composition of assemblages and diversity. Minor climatic events, such as the Younger Dryas, Bolling/Allerod and Dansgaard-Oeschger events are defined quite clearly by variations in cyst accumulation rate.

[47] This work has demonstrated that the sedimentary dinoflagellate cyst record does reflect climatic changes in the late Quaternary on the California Margin, and it opens the door for more detailed, high-resolution studies at appropriate sites elsewhere. Such work should strive to produce quantitative reconstructions of sea-surface temperature and other important paleoenvironmental parameters. But so doing will require significant enhancement of the modern surface-sediment calibration data set for dinoflagel-

late cyst assemblages, and its extension to the temperate zone along the Pacific coast of North America. This stands as a priority for future work.

[48] **Acknowledgments.** Sediment samples were provided by the Ocean Drilling Program (ODP). We thank Bobbi Conard, Phil Rumford,

Bruce Horan, and John Firth (ODP) for their assistance in sampling the core. We gratefully acknowledge R. Behl, W. Berger, E. Emmer, I. Hendy, T. Hill, T. Ivanochko, J. Kennett, and B. Thunell for kindly allowing us access to their data. VP is most grateful to L. Page (University of Victoria) for providing her with a microscope facility. This work was funded by the Fonds pour la Formation de Chercheurs et d'aide à la Recherche du Québec (FCAR) through a grant to VP and the Natural Sciences and Engineering Research Council of Canada (NSERC) through grants to TFP, VP, and AdV.

## References

- Behl, R. J. (1995), Sedimentary facies and sedimentology of the Late Quaternary Santa Barbara Basin (ODP Site 893), *Proc. Ocean Drill. Program Sci. Results*, 146(2), 295–308.
- Behl, R. J., and J. P. Kennett (1996), Brief interstadial events in the Santa Barbara Basin, NE Pacific, during the past 60 kyr, *Nature*, 379, 243–246.
- Dale, B. (1976), Cyst formation, sedimentation, and preservation: Factors affecting dinoflagellate assemblages in recent sediments from Trondheimsfjord, Norway, *Rev. Palaeobot. Palynol.*, 22, 39–60.
- Dale, B. (1996), Dinoflagellate cyst ecology: Modeling and geological applications, in *Palynology: Principles and Applications*, vol. 3, edited by J. Jansonius and D. C. McGregor, pp. 1249–1275, AASP Found., Salt Lake City, Utah.
- de Vernal, A., and T. F. Pedersen (1997), Micro-paleontology and palynology of core PAR87A-10. A 23,000 year record of paleoenvironmental changes in the Gulf of Alaska, northeast North Pacific, *Paleoceanography*, 12, 821–830.
- de Vernal, A., J.-L. Turon, and J. Guiot (1994), Dinoflagellate cyst distribution in high latitude environments and quantitative reconstruction of sea-surface temperature, salinity and seasonality, *Can. J. Earth Sci.*, 31, 48–62.
- de Vernal, A., et al. (2001), Dinoflagellate cyst assemblages as tracers of sea-surface conditions in the northern North Atlantic, Arctic and sub-Arctic seas: The new n = 677 data base and its application for quantitative paleoceanographic reconstruction, *J. Quat. Sci.*, 16(7), 681–698.
- de Vernal, A., et al. (2005), Reconstruction of sea-surface conditions at middle to high latitudes of the Northern Hemisphere during the Last Glacial Maximum (LGM) based on dinoflagellate cyst assemblages, *Quat. Sci. Rev.*, 24, 897–924.
- Doose, H., F. G. Prahm, and M. W. Lyle (1997), Biomarker temperature estimates for modern and last glacial surface waters of the California Current system between 33° and 42°N, *Paleoceanography*, 12, 615–622.
- Emery, K. O. (1960), *The Sea Off Southern California*, 366 pp., John Wiley, Hoboken, N. J.
- Gardner, J. V., and P. Dartnell (1995), Centennial-scale Late Quaternary stratigraphies of carbonate and organic carbon from the Santa Barbara Basin, Hole 893A, and their paleoceanographic significance, *Proc. Ocean Drill. Program Sci. Results*, 146(2), 103–124.
- Head, M. J. (1996), Modern dinoflagellate cysts and their biological affinities, in *Palynology: Principles and Applications*, vol. 3, edited by J. Jansonius and D. C. McGregor, pp. 1197–1248, AASP Found., Salt Lake City, Utah.
- Head, M. J., R. Harland, and J. Matthiessen (2001), Cold marine indicators of the late Quaternary: The new dinoflagellate cyst genus *Islandinium* and related morphotypes, *J. Quat. Sci.*, 16, 621–636.
- Hendy, I. L., and J. P. Kennett (1999), Latest Quaternary North Pacific surface-water responses imply atmosphere-driven climate instability, *Geology*, 27, 291–294.
- Hendy, I. L., and J. P. Kennett (2000), Dansgaard-Oeschger cycles and the California Current System planktonic foraminiferal response to rapid climate change in Santa Barbara Basin, Ocean Drilling Program Hole 893A, *Paleoceanography*, 15, 30–42.
- Hendy, I. L., J. P. Kennett, E. B. Roark, and B. L. Ingram (2002), Apparent synchronicity of submillennial scale climate events between Greenland and Santa Barbara Basin, California from 30–10 ka, *Quat. Sci. Rev.*, 21, 1167–1184.
- Herbert, T. D., M. Yasuda, and C. Burnett (1995), Glacial-interglacial sea surface temperature record as inferred from alkenone unsaturation indices, Site 893, Santa Barbara Basin, in *Proc. Ocean Drill. Program Sci. Results*, edited by J. P. Kennett, J. G. Baldauf, and M. Lyle, pp. 257–264.
- Hickey, B. M. (1998), Coastal oceanography of western North America from the tip of Baja California to Vancouver Island; Coastal segment, *Sea*, 11, 345–393.
- Huyer, A., and R. L. Smith (1974), A subsurface ribbon of cool water over the continental shelf off Oregon, *J. Phys. Oceanogr.*, 4, 381–391.
- Ivanochko, T. S., and T. F. Pedersen (2004), Determining the influences of late Quaternary ventilation and productivity variations on Santa Barbara Basin sedimentary oxygenation: A multi-proxy approach, *Quat. Sci. Rev.*, 23, 467–480.
- Kumar, A., and T. Patterson (2002), Dinoflagellate cyst assemblages from Effingham Inlet, Vancouver Island, British Columbia, Canada, *Palaeogeogr. Palaeoclimatol. Palaeoecol.*, 180, 187–206.
- Lentin, J. K., and G. L. Williams (1993), *Fossil Dinoflagellates: Index to Genera and Species*, 1993 ed., *Contrib. Ser.*, vol. 28, 864 pp., Am. Assoc. of Stratigr. Palynol., Houston, Tex.
- Lewis, J., J. D. Dodge, and A. J. Powell (1990), Quaternary dinoflagellate cysts from the upwelling system offshore Peru, Hole 686B, ODP Leg 112, *Proc. Ocean Drill. Program Sci. Results*, 112, 323–327.
- Lynn, R. J., and J. J. Simpson (1987), The California current system: The seasonal variability of its physical characteristics, *J. Geophys. Res.*, 92, 12,947–12,966.
- Marret, F. (1993), Les effets de l'acétolyse sur les assemblages de kystes de dinoflagellés, *Palynoscience*, 2, 267–272.
- Marret, F., A. de Vernal, D. McDonald, and T. Pedersen (2001), Middle Pleistocene to Holocene palynostratigraphy of ODP Site 887 in the Gulf of Alaska, northeast North Pacific, *Can. J. Earth Sci.*, 38, 373–386.
- Mudie, P. J., A. Rochon, and E. Levac (2002), Palynological records of red tide-producing species in Canada: Past trends and implications for the future, *Palaeogeogr. Palaeoclimatol. Palaeoecol.*, 180, 159–186.
- Pavlova, Y. V. (1966), Seasonal variations of the California current, *Oceanology*, 6, 806–814.
- Pospelova, V. (2005), Dinoflagellate cysts in surface sediments across the northeast Pacific continental shelf in relation to sea-surface temperature, salinity, productivity, and coastal upwelling, paper presented at First International Workshop on Taxonomy of Modern Dinoflagellates in the Pacific, Inst. for East China Sea Res., Nagasaki Univ., Nagasaki, Japan.
- Pospelova, V., and M. J. Head (2002), *Islandinium brevispinosum*, a new species of organic-walled dinoflagellate cyst from modern estuarine sediments of New England (USA), *J. Phycol.*, 38, 593–601.
- Pospelova, V., G. L. Chmura, W. S. Boothman, and J. S. Latimer (2002), Dinoflagellate cyst records and human disturbance in two neighboring estuaries, New Bedford Harbor and Apponagansett Bay, Massachusetts (USA), *Sci. Total Environ.*, 298, 81–102.
- Pospelova, V., G. L. Chmura, and H. A. Walker (2004), Environmental factors influencing spatial distribution of dinoflagellate cyst assemblages in shallow lagoons of southern New England (USA), *Rev. Palaeobot. Palynol.*, 128(1–2), 7–34.
- Pospelova, V., G. L. Chmura, W. Boothman, and J. S. Latimer (2005), Spatial distribution of modern dinoflagellate cysts in polluted estuarine sediments from Buzzards Bay (Massachusetts, USA) embayments, *Mar. Ecol. Prog. Ser.*, 292, 23–40.
- Prauss, M. (2002), Recent global warming and its influence on marine palynology within the central Santa Barbara Basin, offshore southern California, U.S.A., *Palynology*, 26, 217–238.
- Radi, T., and A. de Vernal (2004), Dinocyst distribution in surface sediments from the northeastern Pacific margin (40–60°N) in relation to hydrographic conditions, productivity and upwelling, *Rev. Palaeobot. Palynol.*, 128, 163–193.
- Reichert, G.-J., and H. Brinkhuis (2003), Late Quaternary *Protoperidinium* cysts as indicators of paleoproductivity in the northern Arabian Sea, *Mar. Micropaleontol.*, 49(4), 303–315.
- Rochon, A., A. de Vernal, J.-L. Turon, J. Matthiessen, and M. J. Head (1999), *Distribution of Recent Dinoflagellate Cysts in Surface Sediments From the North Atlantic*

- Ocean and Adjacent Seas in Relation to Sea Surface Parameters, Contrib. Ser.*, vol. 35, 150 pp., Am. Assoc. of Stratigr. Palynol., Houston Tex.
- Stein, R., and F. R. Rack (1995), A 160,000 years high-resolution record of quantity and composition of organic carbon in the Santa Barbara Basin (ODP-Site 893), *Proc. Ocean Drill. Program Sci. Results*, 146(2), 125–138.
- Stockmarr, J. (1977), Tablets with spores used in absolute pollen analysis, *Pollen Spores*, 13(4), 615–621.
- Taylor, F. J. R. (Ed.) (1987), *The Biology of Dinoflagellates, Bot. Monogr.*, vol. 21, 785 pp., Blackwell Sci., Malden, Mass.
- Wall, D., B. Dale, G. P. Lohman, and W. K. Smith (1977), The environmental and climatic distribution of dinoflagellate cysts in the North and South Atlantic Oceans and adjacent seas, *Mar. Micropaleontol.*, 2, 121–200.
- Zonneveld, K. A. F. (1997), New species of organic walled dinoflagellate cysts from modern sediments of the Arabian Sea (Indian Ocean), *Rev. Palaeobot. Palynol.*, 97, 319–337.
- Zonneveld, K. A. F., and G. A. Brummer (2000), Ecological significance, transport and preservation of organic walled dinoflagellate cysts in the Somali Basin, NW Arabian Sea, *Deep Sea Res. II*, 47, 2229–2256.
- Zonneveld, K. A. F., G. J. M. Versteegh, and G. J. de Lange (1997), Preservation of organic-walled dinoflagellate cysts in different oxygen regimes: A 10,000 year natural experiment, *Mar. Micropaleontol.*, 29, 393–405.
- 
- A. de Vernal, Centre de recherche en géochimie isotopique et en géochronologie (GEOTOP), Université du Québec à Montréal, C.P. 8888, Succursale Centre Ville, Montreal, Quebec H3C 3P8, Canada.
- T. F. Pedersen and V. Pospelova, School of Earth and Ocean Sciences, University of Victoria, Petch 168, P.O. Box 3055 STN CSC, Victoria, British Columbia V8W 3P6, Canada. (vpospe@uvic.ca)